Pergamon

Int. J. Solids Structures Vol. 33, No. 7, pp. 967–976, 1996

0020–7683/96 $15.00 + .00

0020–7683(95)00086–0

APPLICATION OF THE SPLINE PRISM METHOD TO ANALYSE VIBRATION OF THICK CIRCULAR CYLINDRICAL PANELS

T. MIZUSAWA and T. KATO
Department of Construction and Civil Engineering, Daido Institute of Technology, Hakusuicho-40, Minami-ku, Nagoya 457, Japan

(*Received 1 November 1994; in revised form 30 March 1995*)

Abstract—This paper presents an application of the spline prism method to analyse vibration of isotropic, thick circular cylindrical panels with two opposite straight edges simply supported. Three-dimensional spline prism models are formulated by combining B-spline functions with beam eigenfunctions. Because of the orthogonality of the beam functions, three-dimensional problems are reduced to a series of two-dimensional ones. To demonstrate the accuracy and convergence of the semi-numerical method, the results are compared with those obtained by the 3D-elasticity theory and by the first-order shear deformation shell theory. Good convergence and accuracy are obtained. The effects of the ratio of thickness to mean radius, the ratio of length to mean radius and the shallowness angle on the frequencies of the thick cylindrical shell panels with some boundary conditions are analysed.

1. INTRODUCTION

Open cylindrical shells with thin or thick thickness are frequently used as structural components of structures and the vibration characteristics of such shells are important for their design. The problem of cylindrical panels has been analysed by means of thin shell theories (Petyt, 1971; Leissa, 1973; Cheung, 1976; Peng-Cheng *et al.*, 1987; Mizusawa, 1988) and the shear deformation shell theories (Reddy and Liu, 1985; Carrera, 1991). Although extensive studies have been made of isotropic, thick cylinders based on the 3D elasticity theory (Mirsky, 1964; Heyliger and Jilani, 1993), the number of available three-dimensional solutions for isotropic, thick cylindrical panels which have considered all effects such as shear deformation, rotary inertia, extension of the normals and other kinematic effects is limited. Soldatos and Hadjigeorgiou (1990) presented an exact solution of simply supported, circular cylindrical panels based on the 3D-elasticity theory which is a kind of discrete layer method.

On the other hand, the finite element method, as the most powerful and versatile tool of solution for the problem of three-dimensional elastic shells and solids, is now well known and established, the computing costs involved are often of staggering proportions. The semi-analytical methods known as the finite prism method (Zienkiewicz and Too, 1972) and the finite layer method (Cheung and Chakrabarti, 1972) based on the 3D elasticity theory have been developed to reduce the computational requirements of the finite element method. These three-dimensional finite strip models have been used to analyse vibration of isotropic and layered, thick plates (Cheung and Chan, 1981; Mizusawa, 1991).

Recently, Mizusawa and Takagi (1993, 1994) analysed vibration of thick rectangular plates and thick annular sector plates by using the spline prism method which is alternative of the finite prism method developed by Zienkiewicz and Too (1972).

This paper presents an application of the spline prism method to analyse vibration of thick circular cylindrical panels with two opposite straight edges simply supported like a diaphragm condition. To demonstrate the convergence and accuracy of the present method, several examples are solved, and the results are compared with those obtained by the 3D elasticity theory and by the first-order shear deformable shell theory. Stable convergence and good accuracy are obtained using the higher-order spline prism models. The effects of the ratio of thickness to mean radius, t/R_c, the ratio of length to mean radius, L/R_c and the shallowness angle, ϕ, on the frequencies of the thick cylindrical panels with some boundary conditions along the circumferential edges are shown in tabular form.

2. SPLINE PRISM METHOD

In this section, the spline prism method based on the three-dimensional elasticity theory is formulated by coupling B-spline functions with beam eigenfunctions. The thick cylindrical panel is modeled by the spline prism elements as shown in Fig. 1.

It is convenient to introduce the non-dimensional cylindrical co-ordinate systems

$$\xi = (r-R_i)/t, \quad \eta = y/L, \quad \zeta = \theta/\phi \tag{1}$$

in which $t = R_i(\lambda-1)$, $R_c = R_i(\lambda+1)/2$, $\lambda = R_0/R_i$, where t is thickness, ϕ is shallowness angle and L is length of the cylindrical panel. R_i and R_0 are inner and outer radii, respectively.

The displacement functions in a prism element are expressed by the product of basic function series in the cylindrical axis direction and B-spline functions which are known as piecewise polynomials in the circumferential direction as follows:

$$\{d\} = \sum_{l=1}^{r} [S]^{l}_{mn}\{\Delta\}_l, \tag{2}$$

where $\{d\} = \{U, V, W\}^{\mathrm{T}}$ is the displacement vector, in which U, V, W are the displacements in the r, y, θ-directions, respectively, $\{\Delta\}_l = \{\{\delta_{\mathrm{A}}\}_l, \{\delta_{\mathrm{B}}\}_l, \{\delta_{\mathrm{C}}\}_l\}^T$ are the unknown coefficients and $[S]_{mn}$ is given by

$$[S]^{l}_{mn} = \begin{bmatrix} [N]_{mn}Z_l & 0 & 0 \\ 0 & [N]_{mn}Z_l & 0 \\ 0 & 0 & [N]_{mn}\bar{Z}_l \end{bmatrix}, \tag{3}$$

where $[N]_{mn} = [N_{1,k}(\xi)N_{1,k}(\eta), N_{1,k}(\xi)N_{2,k}(\eta), \ldots, Ni_{r,k}(\xi)Ni_{y,k}(\eta)]$, $\{\delta_{\mathrm{A}}\}_l = \{A_{11}, A_{12}, \ldots, Ai_ri_y\}^{\mathrm{T}}_l$, $\{\delta_{\mathrm{B}}\}_l = \{B_{11}, B_{12}, \ldots, Bi_ri_y\}^{\mathrm{T}}_l$, $\{\delta_{\mathrm{C}}\}_l = \{C_{11}, C_{12}, \ldots, Ci_ri_y\}^{\mathrm{T}}_l$, and $i_r = k-1+M_r$, $i_y = k-1+M_y$. $Z_l(\xi)$ and $\bar{Z}_l(\xi)$ are the beam eigenfunctions satisfying a given boundary condition. $N_{m,k}(\xi)$ and $N_{n,k}(\eta)$ are the normalized B-spline functions, where $k-1$ is the degrees of spline functions, and M_r and M_y are the number of mesh divisions of prism elements in the r- and y-directions, respectively.

In the three-dimensional elasticity theory, the strain components are defined in the non-dimensional co-ordinate system as follows:

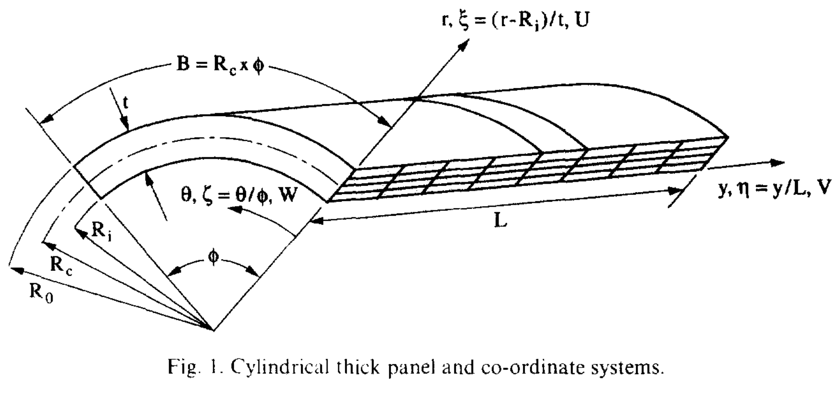

Fig. 1. Cylindrical thick panel and co-ordinate systems.

$$\{\varepsilon\} = \begin{Bmatrix} \varepsilon r \\ \varepsilon y \\ \varepsilon \theta \\ \gamma r y \\ \gamma \theta r \\ \gamma y \theta \end{Bmatrix} = (1/t) \begin{Bmatrix} \partial U/\partial \xi \\ (t/L)(\partial V/\partial \eta) \\ \{U/(\xi + R_i/t) + 1/(\xi + R_i/t)(1/\phi)\,\partial W/\partial \zeta\} \\ \{\partial V/\partial \xi + (t/L)\,\partial U/\partial \eta\} \\ \{\partial W/\partial \xi - W/(\xi + R_i/t) + 1/(\xi + R_i/t)(1/\phi)\,\partial U/\partial \zeta\} \\ \{1/(\xi + R_i/t)(1/\phi)(\partial V/\partial \zeta) + (t/L)(\partial W/\partial \eta)\} \end{Bmatrix} \tag{4}$$

$$= \sum_{l=1}^{r} [B]^l_{mn} \{\Delta\}_l, \tag{5}$$

where the strain matrix, $[B]_{mn}$, of a prism element is defined as follows:

$$[B]^l_{mn} = \sum_{m=1}^{l_\xi} \sum_{n=1}^{l_\eta} (1/t) \begin{bmatrix} \dot{N}_{m,k} N_{n,k} Z_l & 0 & 0 \\ 0 & (t/L) N_{m,k} \dot{N}_{n,k} Z_l & 0 \\ (1/g) N_{m,k} N_{n,k} Z_l & 0 & (1/g\phi) N_{m,k} N_{n,k} \dot{\bar{Z}}_l \\ (t/L) N_{m,k} \dot{N}_{n,k} Z_l & N_{m,k} \dot{N}_{n,k} Z_l & 0 \\ (1/g\phi) N_{m,k} N_{n,k} \dot{Z}_l & 0 & \dot{N}_{m,k} N_{n,k} \bar{Z}_l - (1/g) N_{m,k} N_{n,k} \bar{Z}_l \\ 0 & (1/g\phi) N_{m,k} N_{n,k} \dot{Z}_l & (t/L) N_{m,k} \dot{N}_{n,k} \bar{Z}_l \end{bmatrix}, \tag{6}$$

where $\dot{N}_{m,k} = \partial N_{m,k}(\xi)/\partial \xi$, $\dot{N}_{n,k} = \partial N_{n,k}(\eta)/\partial \eta$, $\dot{Z}_l = \partial Z_l(\zeta)/\partial \zeta$, $\dot{\bar{Z}}_l = \partial \bar{Z}_l(\zeta)/\partial \zeta$ and $g = \xi + 1.0/(\lambda - 1)$.

The stresses are related to the strains for a three-dimensional cylindrical solid by

$$\{\sigma\} = [D]\{\varepsilon\}, \tag{7}$$

where $\{\sigma\} = \{\sigma r \sigma y \sigma \theta \tau r y \tau \theta r \tau y \theta\}^T$ and the elastic matrix becomes

$$[D] = D_0 \begin{bmatrix} 1 & D_1 & D_1 & 0 & 0 & 0 \\ D_1 & 1 & D_1 & 0 & 0 & 0 \\ D_1 & D_1 & 1 & 0 & 0 & 0 \\ 0 & 0 & 0 & D_2 & 0 & 0 \\ 0 & 0 & 0 & 0 & D_2 & 0 \\ 0 & 0 & 0 & 0 & 0 & D_2 \end{bmatrix} \tag{8}$$

in which $D_1 = \nu/(1-\nu)$, $D_2 = (1-2\nu)/2(1-\nu)$, $D_0 = E(1-\nu)/(1+\nu)/(1-2\nu)$, where E and ν are Young's modulus and Poisson ratio, respectively.

The strain energy of the isotropic, three-dimensional cylindrical panel is given by

$$U_p = (t^2 L\phi/2) \int_0^1 \int_0^1 \int_0^1 \{\varepsilon\}^T [D] \{\varepsilon\} \{\xi + 1/(\lambda - 1)\}\, d\xi\, d\eta\, d\zeta$$

$$= (t^2 L\phi/2) \int_0^1 \int_0^1 \int_0^1 \sum_{l=1}^{r} \sum_{s=1}^{q} \{\Delta\}_l^T [B]^{T l}_{mn} [D] [B]^s_{ij} \{\Delta\}_s \{\xi + 1/(\lambda - 1)\}\, d\xi\, d\eta\, d\zeta$$

$$= (1/2) \sum_{l=1}^{r} \sum_{s=1}^{q} \{\Delta\}_l^T [K]_{ls} \{\Delta\}_s, \tag{9}$$

in which $[K]_{ls}$ is the stiffness matrix which is expressed as follows:

$$[K]_{ls} = (t^2 L\phi) \int_0^1 \int_0^1 \int_0^1 [B]_{mn}^{\mathrm{T}l} [D] [B]_{ij}^{s} \{\xi + 1/(\lambda - 1)\} \, \mathrm{d}\xi \, \mathrm{d}\eta \, \mathrm{d}\zeta. \tag{10}$$

The kinetic energy is also written as

$$\begin{aligned} T &= (\rho\omega^2 t^2 L\phi/2) \int_0^1 \int_0^1 \int_0^1 \{U^2 + V^2 + W^2\} \{\xi + 1/(\lambda - 1)\} \, \mathrm{d}\xi \, \mathrm{d}\eta \, \mathrm{d}\zeta \\ &= (\rho\omega^2 t^2 L\phi/2) \int_0^1 \int_0^1 \int_0^1 \sum_{l=1}^{r} \sum_{s=1}^{q} \{\Delta\}_l^{\mathrm{T}} [S]_{mn}^{\mathrm{T}l} [S]_{ij}^{s} \{\Delta\}_s \{\xi + 1/(\lambda - 1)\} \, \mathrm{d}\xi \, \mathrm{d}\eta \, \mathrm{d}\zeta \\ &= (\omega^2/2) \sum_{l=1}^{r} \sum_{s=1}^{q} \{\Delta\}_l^{\mathrm{T}} [M]_{ls} \{\Delta\}_s, \end{aligned} \tag{11}$$

where $[M]_{ls}$ is the mass matrix, and is given by

$$[M]_{ls} = (\rho t^2 L\phi) \int_0^1 \int_0^1 \int_0^1 [S]_{mn}^{\mathrm{T}l} [S]_{ij}^{s} \{\xi + 1/(\lambda - 1)\} \, \mathrm{d}\xi \, \mathrm{d}\eta \, \mathrm{d}\zeta \tag{12}$$

in which ρ is the mass density of the material and ω is the circular frequency (rad s^{-1}).

To deal with arbitrary boundary conditions along the two opposite circumferential edges ($\eta = \eta i_c$), the method of artificial springs (Mizusawa *et al.*, 1993) is used. According to this method, four types of springs, α, β, δ and γ corresponding to displacements, U, V, W, $\partial U/\partial \eta$, respectively, are introduced at each boundary face of the panel.

The energy contribution, U_b due to these springs is given by

$$U_b = (\phi t^2/2) \sum_{i_c=1}^{N_c} \int_0^1 \int_0^1 \{\alpha U^2 + \beta V^2 + \delta W^2 + \gamma(\partial U/\partial \eta)^2\} \{\xi + 1/(\lambda - 1)\} \, \mathrm{d}\xi \, \mathrm{d}\zeta | \eta = \eta \mathrm{i}_c. \tag{13}$$

The functional of the thick cylindrical panel, Π is expressed as follows:

$$\Pi = U_p + U_b - T. \tag{14}$$

By substituting eqn (2) into eqn (14) and using the principle of minimum potential energy, the coefficients $\{\Delta\}_s$ are determined as follows:

$$\partial \Pi / \partial \{\Delta\}_l^{\mathrm{T}} = \sum_{l=1}^{r} \sum_{s=1}^{q} ([K]_{ls} - \omega^2 [M]_{ls}) \{\Delta\}_s = 0. \tag{15}$$

The matrices of $[K]_{ls}$ and $[M]_{ls}$ are given by

$$[K]_{ls} = \begin{bmatrix} [K_{UU}] & [K_{UV}] & [K_{UW}] \\ [K_{VU}] & [K_{VV}] & [K_{VW}] \\ [K_{WU}] & [K_{WV}] & [K_{WW}] \end{bmatrix}_{ls}, \quad [M]_{ls} = \begin{bmatrix} [M_{UU}] & 0 & 0 \\ 0 & [M_{VV}] & 0 \\ 0 & 0 & [M_{WW}] \end{bmatrix}_{ls}. \tag{16}$$

If the two opposite straight edges are simply supported edges ($U = V = \partial V/\partial \zeta = 0$), the basic functions in eqn (2) can be given by

$$Z_l(\zeta) = \sin(l\pi\zeta), \quad \bar{Z}_l(\zeta) = \cos(l\pi\zeta); \quad l = 1, 2, \ldots, r. \tag{17}$$

The properties of orthogonality result in matrices which have no coupling between the different terms and therefore a term by term analysis can be carried out. Thus, the solution of the cylindrical panel with the two opposite edges simply supported is given by

$$\sum ([K]_{ll} - \omega^2 [M]_{ll}) \{\Delta\}_l = 0. \tag{18}$$

In eqn (18), the submatrices of $[K_{ll}]$ and $[M_{ll}]$ are presented in the Appendix. The order of the submatrices is expressed by $3 \times (k-1+M_r) \times (k-1+M_y)$, where $k-1$ is the degree of the B-spline functions, and M_r and M_y are the number of mesh divisions in the r- and y-direction, respectively.

A family of prism models can be generated, corresponding to different degrees of B-spline interpolation across a prism. To perform the integrations required in determining $[K]_{ll}$ and $[M]_{ll}$, analytical (full) integration is always used.

3. NUMERICAL EXAMPLES AND DISCUSSION

Natural frequencies of isotropic, thick circular cylindrical panels are solved to illustrate the convergence and accuracy of the three-dimensional spline prism method which is an alternative to the finite prism method. The two opposite straight edges along the y-direction are assumed to be simply supported and the other two circumferential edges may be arbitrary boundary conditions. For the definition of the boundary conditions along the face of edges, SS-CF, for example, identifies a cylindrical panel with the edges $\zeta = 0$, $\zeta = 1$, $\xi = 0$, $\xi = 1$ having simply supported, simply supported, clamped and free boundary conditions, respectively. A frequency parameter, $n^* = \omega t \sqrt{(\rho/E)}$ is used in the calculations in which t is the thickness of the cylindrical panel.

Table 1 shows the convergence study of the first six natural frequency parameters, $n^* = \omega t \sqrt{(\rho/E)}$ of simply supported cylindrical panels ($\phi = 45°$, $L/R_c = 1.0$ and $\nu = 0.3$) for the different degrees of B-spline functions, $k-1$ and the number of prism elements, $M_r = M_y$. It is seen that stable convergence is obtained with an increase in the degree of spline functions and in the number of prism elements. The higher-order prism model is shown to be rapidly convergent. Therefore, $k-1 = 3$, and $M_r = M_y = 10$ are used in the next examples.

Table 1. Convergence study of frequency parameter, $n^* = \omega t \sqrt{(\rho/E)}$ of simply supported cylindrical shell panels; $\phi = 45°$, $L/R_c = 1.0$ and $\nu = 0.3$

t/R_i ($\lambda = R_0/R_i$)	$k-1$	$M_r = M_y$	Mode 1	2	3	4	5	6
	2	4	0.079001	0.17530	0.19589	0.24817	0.27350	0.32129
0.1		8	0.078837	0.16545	0.19582	0.24817	0.26763	0.28525
(1.1053)		10	0.078832	0.16524	0.19582	0.24817	0.26751	0.28327
		12	0.078830	0.16517	0.19582	0.24816	0.26747	0.28268
	3	4	0.078831	0.16574	0.19582	0.24817	0.26782	0.29533
		8	0.078828	0.16512	0.19582	0.24816	0.26743	0.28236
		10	0.078827	0.16512	0.19582	0.24815	0.26743	0.28225
		12	0.078827	0.16512	0.19582	0.24814	0.26743	0.28223
	2	4	0.78343	0.99213	1.2880	1.4071	1.6597	1.8848
0.4		8	0.78294	0.99212	1.2876	1.3907	1.6582	1.8666
(1.5000)		10	0.78292	0.99212	1.2876	1.3903	1.6581	1.8662
		12	0.78291	0.99211	1.2876	1.3902	1.6581	1.8660
	3	4	0.78292	0.99212	1.2876	1.3913	1.6581	1.8675
		8	0.78291	0.99212	1.2876	1.3900	1.6581	1.8659
		10	0.78291	0.99212	1.2876	1.3900	1.6581	1.8659
		12	0.78291	0.99212	1.2876	1.3900	1.6581	1.8659

To demonstrate the accuracy of the present method, the first four natural frequency parameters, $n^* = \omega L\sqrt{\{\rho(1-\nu)/E\}}$ of a simply supported cylindrical panels are compared with those calculated by the analytical method based on 3D-elasticity theory (Soldatos *et al.*, 1990) in Table 2. It is seen that excellent agreement is obtained.

Table 3 shows the effect of t/R_c on the first six frequency parameters, $n^* = \omega t\sqrt{(\rho/E)}$ of simply supported cylindrical panels ($\phi = 45°$, $L/R_c = 1.0$ and $\nu = 0.3$). The ratio of thickness to mean radius, t/R_c varies from 0.05 to 0.4. The results are also compared with those calculated by the spline strip method (Mizusawa *et al.*, 1994) based on the first-order shear deformable Sanders' shell theory. It is observed that for small ratio of thickness to mean radius, t/R_c, both approaches yield a good agreement. The discrepancy began to widen as the thickness increased. This is attributed to the effect of thickness direction such as high-order shear deformation and thickness deformation to be essential to thick shells.

Table 4 shows the effect of shallowness angle, ϕ on the first six frequency parameters, $n^* = \omega t\sqrt{(\rho/E)}$ of simply supported cylindrical thick panels ($L/R_c = 1.0$, $\lambda = 1.2222$ and $\nu = 0.3$). The angle of ϕ varies from 30° to 90°. The present results are compared with those obtained by the spline strip method (Mizusawa *et al.*, 1994) based on the first-order shear deformation shell theory. To evaluate the adaptability of the first-order shear deformable Sanders' shell theory for thick cylindrical panels, the ratios of t/L and t/B are presented in the table. It is found that the frequency parameters depend on the thickness parameters of t/L and t/B, which are ratios of thickness to panel length and thickness to cylindrical panel width, respectively. The larger value of the thickness ratio is a dominate parameter to assess the accuracy and reliability of solutions obtained by shell theories.

Table 2. Comparison of the natural frequencies, $n^* = \omega L\sqrt{\{\rho(1+\nu)/E\}}$ of simply supported circular cylindrical panel; $\nu = 0.3$

$\phi(°)$	L/R_c	t/R_c	R_o/R_i	t/L	Modes 1st	2nd	3rd	4th
30	0.517638	0.1	1.105263	0.193185	1.20328	3.14682	5.25541	5.76108
					1.20325†	3.14682	5.25539	5.76102
		0.3	1.352941	0.579556	2.21292	3.14991	4.62052	5.00861
					2.21292†	3.14991	4.62052	5.00858
60	1.0	0.1	1.105263	0.1	0.80964	3.15331	5.23679	5.78461
					0.80963†	3.15331	5.23675	5.78457
		0.3	1.352941	0.3	1.52806	3.16159	5.11234	5.56169
					1.52805†	3.16159	5.11234	5.56168
90	1.414214	0.1	1.105263	0.070711	0.89466	3.15294	5.15984	5.78911
					0.89464†	3.15292	5.15983	5.78907
		0.3	1.352941	0.212132	1.21998	3.15903	5.09827	5.57240
					1.21997†	3.15903	5.09826	5.57237

† The results are calculated by Soldatos and Hadjigeorgiou (1990) using the analytical method.

Table 3. The effect of t/R_c on the first six frequency parameters, $n^* = \omega t\sqrt{(\rho/E)}$ of simply supported cylindrical panels; $\phi = 45°$, $L/R_c = 1.0$ and $\nu = 0.3$

t/R_c ($\lambda = R_o/R_i$)	Theory	Mode 1	2	3	4	5	6
0.05 (1.0513)	3D-elasticity	0.025805	0.053135	0.053635	0.075980	0.086038	0.10829
	FSDT Sanders†	0.025814	0.053193	0.053230	0.075857	0.086062	0.097399
0.1 (1.1053)	3D-elasticity	0.078827	0.16512	0.19582	0.24815	0.26743	0.28225
	FSDT Sanders†	0.078696	0.16493	0.19462	0.19469	0.26561	0.28131
0.2 (1.2222)	3D-elasticity	0.26125	0.49675	0.51400	0.62920	0.64313	0.81546
	FSDT Sanders†	0.25852	0.38854	0.51142	0.61838	0.64502	0.77704
0.4 (1.5000)	3D-elasticity	0.78291	0.99212	1.2876	1.3900	1.6581	1.8659
	FSDT Sanders†	0.75754	0.77049	1.3031	1.3533	1.5400	1.6059

† FSDT Sanders is the first-order shear deformable Sanders' shell theory (Mizusawa *et al.*, 1994).

Table 4. The effect of shallowness angle, ϕ on the frequency parameters, $n^* = \omega t\sqrt{(\rho/E)}$ of simply supported cylindrical panels: $L/R_c = 1.0$, $t/R_c = 0.2$, $\lambda = 1.2222$ and $\nu = 0.3$

ϕ	t/L	t/B		Mode 1	2	3	4	5	6
30	0.2	0.382	3D-elasticity	0.4247	0.6443	0.7447	0.8472	0.9454	1.0862
			FSDT Sanders†	0.3885	0.4184	0.6344	0.7770	0.8492	0.9299
45	0.2	0.255	3D-elasticity	0.2613	0.4969	0.5140	0.6292	0.6431	0.8155
			FSDT Sanders†	0.2585	0.3885	0.5114	0.6184	0.6450	0.7770
60	0.2	0.190	3D-elasticity	0.2101	0.3726	0.4247	0.4741	0.5537	0.6443
			FSDT Sanders†	0.2089	0.3885	0.4184	0.4713	0.5553	0.6344
90	0.2	0.127	3D-elasticity	0.1931	0.2485	0.3613	0.4247	0.4470	0.4768
			FSDT Sanders†	0.1932	0.2585	0.3885	0.4184	0.4461	0.4778

† FSDT Sanders is the first-order shear deformable Sanders' shell theory (Mizusawa *et al.*, 1994).

Table 5. The effect of L/R_c on the first six frequency parameters $n^* = \omega t\sqrt{(\rho/E)}$ of simply supported cylindrical panels: $\phi = 45°$, $t/R_c = 0.2$ and $\lambda = 1.2222$ and $\nu = 0.3$

L/R_c	Theory	Mode 1	2	3	4	5	6
0.25	3D-Elasticity	0.49676	0.99224	1.2011	1.4030	1.4852	1.6381
	FSDT Sanders†	1.1823	1.3741	1.5538	1.6358	1.6667	1.8550
0.5	3D-Elasticity	0.49675	0.51640	0.81546	0.93198	0.99224	1.2011
	FSDT Sanders†	0.51142	0.77704	0.80034	0.93371	1.1823	1.2022
1.0	3D-Elasticity	0.26125	0.49676	0.51400	0.62920	0.64313	0.81546
	FSDT Sanders†	0.25852	0.38854	0.51142	0.61838	0.64502	0.77704
2.0	3D-Elasticity	0.18440	0.26125	0.37683	0.49674	0.51661	0.54009
	FSDT Sanders†	0.18277	0.19427	0.25852	0.37326	0.38854	0.51142
4.0	3D-Elasticity	0.166300	0.18440	0.21664	0.26136	0.31611	0.38062
	FSDT Sanders†	0.097136	0.16442	0.18227	0.19427	0.21421	0.25852

† FSDT Sanders is the first-order shear deformable Sanders' shell theory (Mizusawa *et al.*, 1994).

Table 5 shows the effect of L/R_c on the first six frequency parameters of simply supported cylindrical panels ($\phi = 45°$, $t/R_c = 0.2$, $\lambda = 1.22222$ and $\nu = 0.3$). The results are also compared with those obtained by the spline strip method (Mizusawa *et al.*, 1994) based on the first-order shear deformable Sanders' shell theory. It is observed that the results calculated by the two approaches show a difference due to the assumptions of a simply supported boundary condition. The discrepancy of the frequency parameters calculated by the two approaches shows for larger ($L/R_c > 2.0$) or shorter ($L/R_c < 0.5$) cylindrical panels.

Table 6(a–d) shows the first six frequency parameters, $n^* = \omega t\sqrt{(\rho/E)}$ of thick cylindrical panels with different shallowness angles, ϕ and t/R_c, having boundary conditions of SS-CC, SS-SS, SS-CF and SS-FF, respectively. The angle of ϕ varies from 30° to 90°, and t/R_c of 0.1, 0.2 and 0.4 are used. It is observed that the frequency parameters increase with increment of t/R_c, and decrease with an increase in the shallowness angles. This is attributed to the effect of thickness of cylindrical panels associated with the influence of shear deformation, thickness deformation and in-plane inertia.

Lastly, Table 7 shows the effect of Poisson ratio, ν, on the first six frequency parameters, $n^* = \omega t\sqrt{(\rho/E)}$ of cylindrical panels ($\phi = 45°$, $t/R_c = 0.2$, $L/R_c = 1.0$ and $\lambda = 1.22222$) with some boundary conditions. Poisson ratios of $\nu = 0.0$, 0.15 and 0.3 are used. The frequency parameters decrease with increment of Poisson ratio, and the effect of Poisson ratio on the frequency parameters is significant for the cylindrical panel with free edges.

4. CONCLUDING REMARKS

This paper presents an application of the spline prism method based on the 3D-elasticity theory to analyse the frequencies of isotropic, circular cylindrical thick panels

Table 6. The first six frequency parameters, $\omega^* = \omega t\sqrt{(\rho/E)}$ of cylindrical thick panels with some boundary conditions along the circumferential edges; $L/R_c = 1.0$ and $\nu = 0.3$

(a) SS-CC

t/R_c ($\lambda = R_o/R_i$)	ϕ(°)	t/L	t/B	Mode 1	2	3	4	5	6
0.1	30		0.191	0.1398	0.2349	0.3610	0.3795	0.4471	0.4506
(1.1053)	60	0.1	0.0955	0.09254	0.1398	0.1935	0.2349	0.2436	0.3188
	90		0.0637	0.09557	0.09976	0.1398	0.1901	0.2016	0.2046
0.2	30		0.382	0.4533	0.6917	0.9049	0.9941	1.096	1.155
(1.2222)	60	0.2	0.191	0.2741	0.4533	0.5549	0.6857	0.6917	0.7276
	90		0.127	0.2609	0.3134	0.4533	0.5382	0.5788	0.5853
0.4	30		0.765	1.240	1.687	1.844	2.202	2.360	2.580
(1.5000)	60	0.4	0.382	0.7346	1.240	1.327	1.412	1.418	1.687
	90		0.255	0.6675	0.8645	1.148	1.240	1.297	1.323

(b) SS-SS

t/R_c ($\lambda = R_o/R_i$)	ϕ(°)	t/L	t/B	Mode 1	2	3	4	5	6
0.1	30		0.191	0.1258	0.2053	0.3211	0.3722	0.3757	0.4232
(1.1053)	60	0.1	0.0955	0.07099	0.1258	0.1546	0.1861	0.2053	0.2366
	90		0.0637	0.07740	0.07883	0.1241	0.1258	0.1497	0.1651
0.2	30		0.382	0.4247	0.6443	0.7447	0.8472	0.9454	1.086
(1.2222)	60	0.2	0.191	0.2101	0.3726	0.4247	0.4741	0.5537	0.6443
	90		0.127	0.1931	0.2485	0.2613	0.4247	0.4470	0.4768
0.4	30		0.764	1.198	1.476	1.680	1.685	2.166	2.312
(1.500)	60	0.4	0.382	0.6233	0.7463	1.110	1.198	1.287	1.476
	90		0.255	0.4986	0.5298	0.7829	0.9560	0.9921	1.198

(c) SS-CF

($\lambda = R_o/R_i$)	ϕ(°)	t/L	t/B	Mode 1	2	3	4	5	6
0.1	30		0.191	0.1042	0.1586	0.2557	0.3485	0.3569	0.3826
(1.1053)	60	0.1	0.0955	0.03851	0.1042	0.1070	0.1586	0.2036	0.2080
	90		0.0637	0.04078	0.05208	0.1042	0.1087	0.1154	0.1586
0.2	30		0.382	0.3601	0.5033	0.6986	0.7630	0.9932	1.043
(1.2222)	60	0.2	0.191	0.1224	0.3100	0.3601	0.4225	0.5034	0.6013
	90		0.127	0.09827	0.1842	0.2914	0.3555	0.3589	0.3601
0.4	30		0.764	1.043	1.266	1.494	1.834	2.013	2.292
(1.5000)	60	0.4	0.382	0.3887	0.7612	0.9377	1.043	1.235	1.266
	90		0.255	0.2650	0.5833	0.6875	0.7975	0.8958	0.9338

(d) SS-FF

($\lambda = R_o/R_i$)	ϕ(°)	t/L	t/B	Mode 1	2	3	4	5	6
0.1	30		0.191	0.09717	0.1152	0.1780	0.2741	0.3291	0.3818
(1.1053)	60	0.1	0.0955	0.02218	0.03448	0.09717	0.1152	0.1227	0.1533
	90		0.0637	0.007896	0.01385	0.04212	0.05789	0.09717	0.1092
0.2	30		0.382	0.3404	0.3910	0.5581	0.6530	0.7770	0.8266
(1.2222)	60	0.2	0.191	0.08509	0.1242	0.3150	0.3404	0.3626	0.3910
	90		0.127	0.03090	0.05028	0.1573	0.2059	0.2264	0.3289
0.4	30		0.764	1.007	1.072	1.348	1.372	1.672	1.965
(1.5000)	60	0.4	0.382	0.3021	0.3709	0.6883	0.9791	1.007	1.072
	90		0.255	0.1169	0.1551	0.4997	0.5224	0.6011	0.8254

Table 7. The effect of Poisson ratio, ν on frequency parameter, $\omega^* = \omega t\sqrt{(\rho/E)}$ of cylindrical panels; $\phi = 45°$, $L/R_c = 1.0$, $t/R_c = 0.2$ and $\lambda = 1.2222$

Boundary conditions	ν	Mode 1	2	3	4	5	6
SS-FF	0.0	0.18100	0.25382	0.49829	0.52748	0.65390	0.72708
	0.15	0.17603	0.23880	0.47189	0.49479	0.62921	0.69109
	0.3	0.15729	0.20589	0.41234	0.42289	0.55618	0.60113
SS-SS	0.0	0.29864	0.59975	0.65714	0.73323	0.84988	0.96003
	0.15	0.29015	0.57886	0.59635	0.70629	0.77159	0.92083
	0.3	0.26125	0.49676	0.51400	0.62920	0.64313	0.81546
SS-CC	0.0	0.36626	0.69743	0.75499	0.94170	1.0096	1.0456
	0.15	0.35196	0.66496	0.72553	0.87187	0.96264	0.99847
	0.3	0.31340	0.58529	0.64470	0.74208	0.84703	0.88314

with the two opposite straight edges simply supported and the other two of some boundary conditions. The effects of ratio of thickness to radius, t/R_c, ratio of length to radius, L/R_c and shallowness angle, ϕ on the frequency parameters are analysed, and the results are compared with those calculated by the analytical method based on the 3D-elasticity theory and by the spline strip method based on the first-order shear deformable Sanders' shell theory.

The main conclusions of the present work can be summarized as follows:

(1) The higher-order spline prism models show the highest efficiency on the rapid convergence of frequencies.
(2) The frequency parameters of the circular cylindrical panels are dependent on the ratios of t/R_c, L/R_c, ϕ and boundary conditions.
(3) The present method can be used to predict the frequencies of both thick and thin circular cylindrical panels.
(4) The results predicted by the first-order shear deformable Sanders' shell theory are limited in use by the ratios of ϕ and L/R_c of thick cylindrical panels.
(5) The frequency parameters of circular cylindrical thick panels with some boundary conditions are presented in tabular form, and can serve to validate other methods and finite element models.

Acknowledgements—The results presented in this paper were obtained during the course of a research programme, Grant No. 04650412, supported by the Ministry of Education, Science and Culture of the Japanese Government.

REFERENCES

Carrera, E. (1991). The effects of shear deformation and curvature on buckling and vibrations of cross-ply laminated composite shells. *J. Sound Vibr.* **150**, 405–433.

Cheung, M. S. and Chan, M. Y. T. (1981). Static and dynamic analysis of thin and thick sectorial plates by the finite strip method. *Comput. Structures* **14**, 79–88.

Cheung, Y. K. (1976). *Finite strip method in structural analysis*. Pergamon Press, New York.

Cheung, Y. K. and Chakrabarti, S. (1972). Free vibration of thick, layered rectangular plates by a finite layer method. *J. Sound Vibr.* **21**, 277–284.

Heyliger, P. R. and Jilani, A. (1993). Free vibrations of laminated anisotropic cylindrical shells. *J. Engng Mech., ASCE* **119**, 1062–1077.

Leissa, A. W. (1973). The vibrations of shells. *NASA Rep. SO-288*, NASA, Washington, DC.

Mirsky, I. (1964). Vibrations of orthotropic, thick cylindrical shells. *J. Acoustic Soc. Am.* **36**, 41–51.

Mizusawa, T. (1988). Application of spline strip method to analyse vibration of open cylindrical shells. *Int. J. Numer. Meth. Engng* **26**, 663–676.

Mizusawa, T. (1991). Vibration of thick annular sector plates using semi-analytical methods. *J. Sound Vibr.* **150**, 245–259.

Mizusawa, T. and Takagi, S. (1993). Vibration of thick rectangular plates by using the spline prism method. *J. Struct. Engng, JSCE* **39A**, 1–12.

Mizusawa, T. and Kito, H. (1994). Application of the spline strip method to analyse vibration of cross-ply laminated cylindrical panels. *Proc. Symp. Comput. Meth. Struct. Engng Related Fields* **18**, 337–342.

Peng-Cheng, S. and Jian-Guo, W. (1987). Vibration analyses of flat shells by using B-spline functions. *Comput. Structures* **25**, 1–10.

Petyt, M. (1971). Vibration of curved panels. *J. Sound Vibr.* **15**, 381–395.

Reddy, J. N. and Liu, C. F. (1985). A higher-order shear deformation theory of laminated elastic shells. *Int. J. Engng Sci.* **25**, 319–330.

Soldatos, K. P. and Hadjigeorgiou, V. P. (1990). Three-dimensional solution of the free vibration problem of homogeneous isotropic cylindrical shells and panels. *J. Sound Vibr.* **137**, 369–384.

Takagi, S. and Mizusawa, T. (1994). Vibration of thick annular sector plates by using the spline prism method. *J. Struct. Engng, JSCE* **40A**, 1–12.

Zienkiewicz, O. C. and Too, J. J. M. (1972). The finite prism in analysis of thick simply supported bridge boxes. *Proc. Inst. Civil Engineers* **53**, 147–172.

APPENDIX

The sub-matrices in eqns (18) are given as follows:

$$[K_{UU}] = (L\phi D_0)\{I_{mi}^{111}J_{nj}^{00}A_1 + D_1 I_{mi}^{010}J_{nj}^{00}A_1 + D_1 I_{mi}^{100}J_{nj}^{00}A_1$$

$$+ I_{mi}^{00-1}J_{nj}^{00}A_1 + D_2(t/L)^2 I_{mi}^{001}J_{nj}^{11}A_1 + D_2(1/\phi)^2 I_{mi}^{00-1}J_{nj}^{00}A_2\}$$

$$[K_{UV}] = (L\phi D_0)\{D_1(t/L)I_{mi}^{101}J_{nj}^{01}A_1 + D_1(t/L)I_{mi}^{000}J_{nj}^{01}A_1 + D_2(t/L)I_{mi}^{011}J_{nj}^{10}A_1\}$$

$$[K_{UW}] = (L\phi D_0)\{D_1(1/\phi)I_{mi}^{010}J_{nj}^{00}A_3 + (1/\phi)I_{mi}^{00-1}J_{nj}^{00}A_3$$

$$+ D_2(1/\phi)I_{mi}^{010}J_{nj}^{00}A_4 + D_2(1/\phi)I_{mi}^{00-1}J_{nj}^{00}A_4\}$$

$$[K_{VU}] = (L\phi D_0)\{D_1(t/L)I_{mi}^{011}J_{nj}^{10}A_1 + D_1(t/L)I_{mi}^{000}J_{nj}^{10}A_1 + D_2(t/L)I_{mi}^{101}J_{nj}^{01}A_1\}$$

$$[K_{VV}] = (L\phi D_0)\{(t/L)^2 I_{mi}^{001}J_{nj}^{11}A_1 + D_2 I_{mi}^{111}J_{nj}^{00}A_1 + D_2(1/\phi)^2 I_{mi}^{00-1}J_{nj}^{00}A_2\}$$

$$[K_{VW}] = (L\phi D_0)\{D_1(t/L)(1/\phi)I_{mi}^{000}J_{nj}^{10}A_3 + D_2(1/\phi)(t/L)I_{mi}^{000}J_{nj}^{01}A_5\}$$

$$[K_{WU}] = (L\phi D_0)\{D_1(1/\phi)I_{mi}^{010}J_{nj}^{00}A_6 + (1/\phi)I_{mi}^{00-1}J_{nj}^{00}A_6$$

$$+ D_2(1/\phi)I_{mi}^{100}J_{nj}^{00}A_5 + D_2(1/\phi)I_{mi}^{00-1}J_{nj}^{00}A_5\}$$

$$[K_{WV}] = (L\phi D_0)\{D_1(t/L)(1/\phi)I_{mi}^{000}J_{nj}^{01}A_6 + D_2(t/L)(1/\phi)I_{mi}^{000}J_{nj}^{10}A_5\}$$

$$[K_{WW}] = (L\phi D_0)\{(1/\phi)^2 I_{mi}^{00-1}J_{nj}^{00}A_7 + D_2(I_{mi}^{111}J_{nj}^{00}A_8$$

$$+ I_{mi}^{100}J_{nj}^{00}A_8 + I_{mi}^{010}J_{nj}^{00}A_8 - I_{mi}^{00-1}J_{nj}^{00}A_8 + (t/L)^2 I_{mi}^{001}J_{nj}^{11}A_8)\}$$

and

$$[M_{UU}] = (\rho t^2 L\phi)\{I_{mi}^{000}J_{nj}^{00}A_1\}, \quad [M_{VV}] = (\rho t^2 L\phi)\{I_{mi}^{000}J_{nj}^{00}A_1\}$$

$$[M_{WW}] = (\rho t^2 L\phi)\{I_{mi}^{000}J_{nj}^{00}A_8\},$$

in which the integrals I_{mi}^{tuC} and J_{nj}^{tu} are defined as

$$I_{mi}^{tuC} = \int_0^1 N_{m,k}^{(t)}(\xi)N_{i,k}^{(u)}(\xi)\{\xi + 1/(\lambda - 1)\}^C \, d\xi, \quad J_{nj}^{tu} = \int_0^1 N_{n,k}^{(t)}(\eta)N_{n,k}^{(u)}(\eta)\, d\eta,$$

where t and u are the order derivatives of $N_{m,k}(\xi)$ and $N_{n,k}(\eta)$, and C is the order of $\{\xi + 1/(\lambda - 1)\}$. A_i is also given by

$$A_1 = A_8 = 0.5, \quad A_2 = A_7 = (l\pi)^2, \quad A_3 = A_5 = -l\pi \quad \text{and} \quad A_4 = A_6 = l\pi.$$